Synthesis and Characterization of Diblock Copolymer Films Containing Self-Assembled Polyacetylene Structures

Randall S. Saunders,† Robert E. Cohen,*,† and Richard R. Schrock‡

Departments of Chemical Engineering and Chemistry, Massachusetts Institute of Technology, Cambridge, Massachusetts 02139

Received March 13, 1991

ABSTRACT: Ring-opening metathesis polymerization (ROMP) has been performed with a tungsten alkylidene catalyst to make monodisperse block copolymers of norbornene or a 5-((trimethylsiloxy)methyl)-norbornene and a new "Durham" polyacetylene precursor, *p*-dimethoxybenzotricyclo[4.2.2.0^{2,5}]deca-3,7,9-triene. The block copolymers with norbornene showed microphase separation by small-angle X-ray scattering (SAXS) but the morphology was not observable by transmission electron microscopy (TEM). Seven block copolymers with the 5-((trimethylsiloxy)methyl)norbornene were made, varying both molecular weight and percent of each block. Six of these showed microphase separation by SAXS, with morphologies ranging from spherical to cylindrical to lamellar. One cylindrical and all lamellar morphologies were observed by TEM. The lamellar spacing of the diblocks increased with the $^2/_3$ power of the copolymer molecular weight, in good agreement with previously proposed scaling laws for amorphous block copolymer lamellar systems. The six diblocks showing the microphase separation were heat treated to thermally eliminate dimethoxynaphthalene and form block copolymers of 5-((trimethylsiloxy)methyl)norbornene and polyacetylene. Except for the lowest molecular weight sample, all the block copolymers retained their microphase separation as seen by SAXS and TEM, thus creating self-assembled structures of polyacetylene dispersed throughout the derivatized polynorbornene matrix.

Introduction

Incorporating electrically conductive polymers into heterogeneous block copolymers immediately leads to the possibility of producing self-assembled structures containing the conducting material. These structures would be distributed in regular patterns, at a scale as small as several nanometers, throughout the nonconducting matrix. The potential ease of fabrication of such structures makes the self-assembly of the block copolymer morphology[1] an appealing alternative to more laborious techniques such as the Langmuir–Blodgett process[2] or sequential static casting or spin coating.[3] The characteristic spherical, cylindrical, and lamellar morphologies of block copolymers offer the potential of achieving three-, two-, or one-dimensional confinement of the conducting regions. The recently discovered ordered bicontinuous double-diamond morphology[4] offers interesting possibilities for a pseudo "nonconfinement" of the conducting regions, leading to isotropic behavior on a large scale. Long-range ordering of the cylindrical and lamellar morphologies is necessary to obtain anisotropic behavior and has been achieved[5] in nonconducting block copolymers. Long-range ordering of spherical morphology has also been obtained by coaxing the spherical domains into a cubic lattice.[6] All these morphologies, containing the self-assembled conducting regions, could allow for the fabrication of novel dielectric and electrically conductive polymer devices.

A significant amount of morphological characterization has been carried out on heterogeneous block copolymers, and well-tested scaling laws[7] and carefully examined phase diagrams[8,9] reveal the molecular weight and composition dependences of the morphological features of the spherical, cylindrical, and lamellar systems. If such scaling laws and phase diagrams described the behavior of block copolymers containing conducting moieties, they would be very useful design tools for assistance in device fabrication. However, little is known about the morphologies of block copolymers in which an electrically conductive sequence is present. Both graft[10–15] and block[16–22] copolymers containing polyacetylene have been synthesized and some do indeed show self-assembled polyacetylene-rich structures.[13–15,21,22] Except for the work of Aldissi,[22] most of these polymer morphologies are not well controlled and characterized.

In the present paper we discuss our work on the synthesis and molecular and morphological characterization of diblock copolymers containing polyacetylene. The final diblocks were obtained from precursor diblocks that were synthesized by using techniques[23–25] of ring-opening metathesis polymerization (ROMP) using an alkylidene catalyst.[26] These precursor diblocks each contain one sequence of polynorbornene (or a derivatized polynorbornene) and one sequence of a precursor polymer which converts to polyacetylene via a retro-Diels–Alder reaction (the "Durham route"[27] to polyacetylene) upon heating (Figures 1 and 2). Films of the carefully characterized precursor diblocks and the set of polyacetylene-containing diblocks obtained from them were subjected to morphological examination using transmission electron microscopy (TEM) and small-angle X-ray scattering (SAXS).

Experimental Section

Monomers. Norbornene was purchased from Aldrich and purified by distillation over sodium sand. Bis(trifluoromethyl)-tricyclo[4.2.2.0^{2,5}]deca-3,7,9-triene[28] and benzotricyclo[4.2.2.0^{2,5}]-deca-3,7,9-triene[29] were prepared by methods described in the literature. *p*-Dimethoxybenzotricyclo[4.2.2.0^{2,5}]deca-3,7,9-triene was prepared by a modification of an existing literature preparation.[30]

((Trimethylsiloxy)methyl)norbornene. 5-Norbornene-2-methanol (40 g (322 mmol)) (available from Aldrich) and 25.5 g (322 mmol) of pyridine were placed in a 1000-mL round-bottom flask along with 600 mL of anhydrous diethyl ether. The solution was stirred magnetically while 35.0 g (322 mmol) of trimethylsilyl chloride was added over a period of 1 min. A white precipitate of the pyridine hydrochloride salt formed immediately upon addition. The solution was stirred under nitrogen for 24 h, after which the solids were filtered off and washed with more ether. The solvent of the filtrate was removed under reduced pressure, and the product was distilled at 1 Torr, coming over at 75 °C.

† Department of Chemical Engineering.
‡ Department of Chemistry.

0024-9297/91/2224-5599$02.50/0

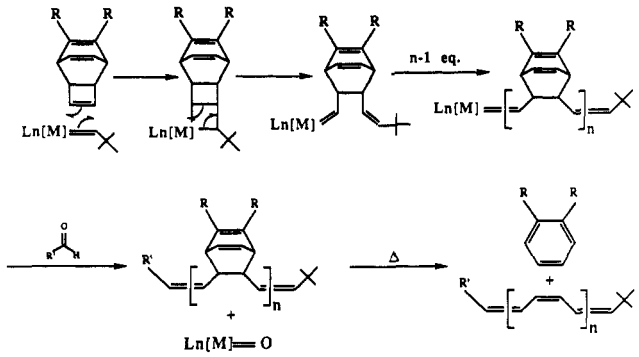

Figure 1. The controlled "Durham route" to polyacetylene.

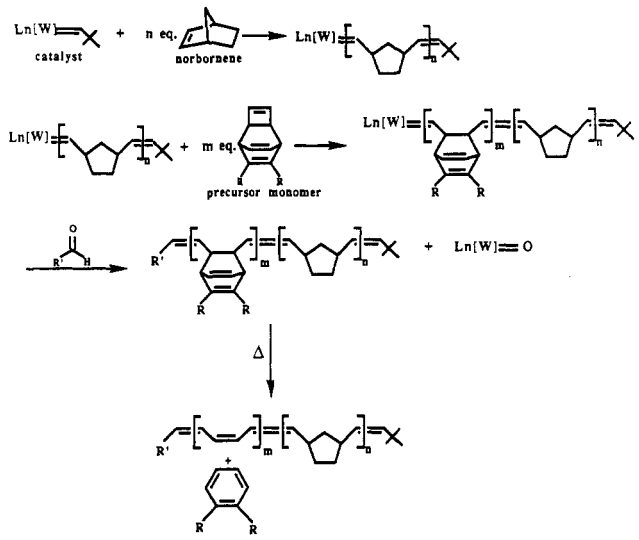

Figure 2. Synthesis of diblocks of polynorbornene and the precursor polymer and their conversion to diblocks of polynorbornene and polyacetylene. Ln[W] represents the catalyst containing a tungsten metal center and attached ligands.

A total of 59 g (94%) of the product was recovered in this way. Further purification was performed by stirring the product over a sodium/potassium alloy overnight and redistilling, thereby removing any impurities that could hinder the catalyst activity. The ^{1}H NMR spectrum of this compound was complicated by the endo–exo isomer mixture of the initial reactant.

Polymerizations. All polymerizations were performed in a Vacuum Atmospheres drybox with toluene as a solvent. Toluene was purified by distilling first over calcium hydride, then over molten sodium (after refluxing at least 5 days), and then storing over a sodium/potassium alloy. A typical procedure is as follows: three solutions are made—solution a is prepared by dissolving 12 mg of catalyst (2.09×10^{-5} mol) in 1 mL of toluene, solution b is prepared by dissolving the desired amount of ((trimethylsiloxy)methyl)norbornene in 19 mL of toluene, and solution c is prepared by dissolving the desired amount of precursor monomer in 4 mL of toluene. Solution a is added to a stirring solution b, and the mixture is allowed to stir for 45 min. At this point a small portion is removed and capped for GPC analysis. Solution c is then added, and the mixture is allowed to stir for another 30 min. At this time, 15 μL of benzaldehyde is added to terminate the living ends, and the solution is stirred for another 5 min. The polymer solution is diluted with enough dichloromethane to make a 3 wt % polymer solution. This solution is then added slowly to methanol, and the precipitated polymer is filtered and dried overnight on a high-vacuum line.

Molecular Characterization. Relative molecular weights and molecular weight distributions of the first block and total diblock of each sample were determined by gel permeation chromatography (GPC) using a series of four Waters Ultrastyragel columns (10^6, 10^4, 10^3, and 500 Å) connected to a differential refractometer. The mobile phase was dichloromethane at a flow rate of 1 mL/min. The percentage of each block in the diblocks

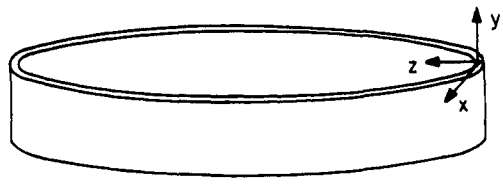

Figure 3. Typical polymer film made from spin casting.[31] Axes are included to aid in SAXS descriptions.

Table I
Precursor Diblock Systems

system	matrix block monomer	precursor monomer	diblock copolymer
A.			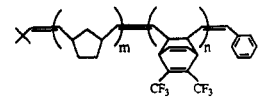
B.			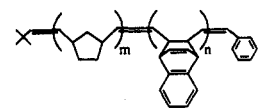
C.		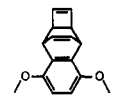	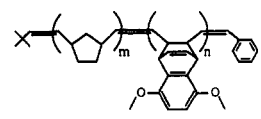
D.	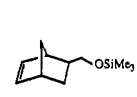	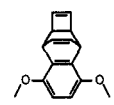	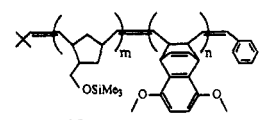

was determined by ^{1}H NMR on an IBM NR/200AF and by differential scanning calorimetry (DSC) on a Perkin-Elmer DSC series 7, and the results compared favorably with stoichiometry.

Film Preparation. Films of diblocks 1–7 (Table II) were made by dissolving 1 g of polymer in 40 mL of THF, putting this solution in a cup, and rotating the cup at high rpm (spin casting technique[31]). The solvent evaporated slowly at room temperature, and over the course of about 20 h, a thin polymer film remained on the wall of the cup. For purposes of describing various SAXS patterns, the x direction is tangential to the spin direction, the y direction pertains to the direction going from the bottom of the cup to the top, and the z direction is the radial direction pointing to the center of the cup from the wall (Figure 3). After the film is spin cast, it is annealed for 24 h at 50 °C in a vacuum oven.

Precursor Conversion to Polyacetylene. A portion of each film was heated in air (for any future electrical studies this step must be performed in an inert atmosphere) at atmospheric pressure on a hot plate at 130 °C for 10 min. Each precursor eliminates an aromatic unit. A small portion of this aromatic substance escapes, but most remains in the film and acts as a diluent.

Morphological Characterization. Morphologies of the prepared films were examined by TEM with a Philips EM300, operating at 100 kV, and by SAXS using a Rigaku instrument with a 1.54-Å Cu Kα rotating-anode point source, Charles Supper double mirror focusing optics, and a Nicolet two-dimensional detector. Ultrathin samples for the TEM were prepared with an LKB Ultratome III Model 8800. The X-ray fluorescence experiment was performed on a STEM (VG-HB5, operating voltage 100 kV).

Results

Four diblock systems were synthesized, all involving norbornene or a (trimethylsiloxy)methyl-substituted norbornene and a precursor monomer (Table I). Systems C and D have been more thoroughly studied, with system D being the most extensively studied, for reasons that will be discussed below.

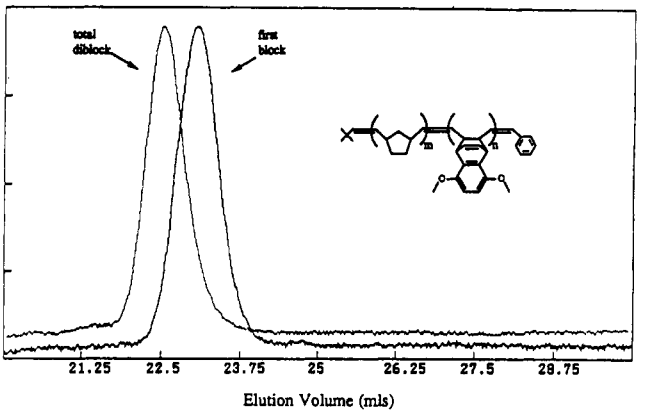

Figure 4. GPC trace of diblock system C in Table I; molecular weight 37 500, 33 wt % precursor block/67 wt % polynorbornene.

Figure 5. SAXS pattern of diblock system C in Table I; molecular weight 37 500, 33 wt % precursor block/67 wt % polynorbornene.

Table II
Molecular Characterization Results for Diblocks of System D: NMR, DSC, and GPC Results

diblock	mol wt	stoichiometric wt, %	wt % by DSC	wt % by NMR	av of wt % by DSC and NMR	polydispersity by GPC
1	48 000	8	7.4	9	8.2	1.74
2	48 000	15	15.5	18	16.8	1.23
3	48 000	28	27.7	27	27.4	1.07
4	48 000	50	51.3	53	52.2	1.04
5	35 000	50	50.9	51	51.0	1.04
6	20 000	50	51.2	47	49.1	1.06
7	10 000	50	56.9	45	51.0	1.10

One diblock of system C was made consisting of a norbornene block of molecular weight 25 000 and a precursor block of molecular weight 12 500. A gel permeation chromatography (GPC) trace of the first block and total diblock are shown in Figure 4. A film of this diblock, spin cast from a THF/hexane mixture at room temperature, was analyzed by small-angle X-ray scattering (SAXS), and the x direction results are shown in Figure 5. The y direction gave a similar pattern, and the z direction gave no pattern. Staining this diblock for transmission electron microscopy (TEM) was not successful, and therefore no TEM results are available.

Seven diblocks of system D were prepared and analyzed by GPC. Spin cast samples of these diblocks have been analyzed by NMR, DSC, SAXS, TEM, and STEM, and most of the results are summarized in Tables II (DSC, NMR, and GPC) and III (SAXS). These seven diblocks consist of one series of constant molecular weight and varying composition (diblocks 1–4) and a second series of constant composition but varying molecular weight (diblocks 4–7).

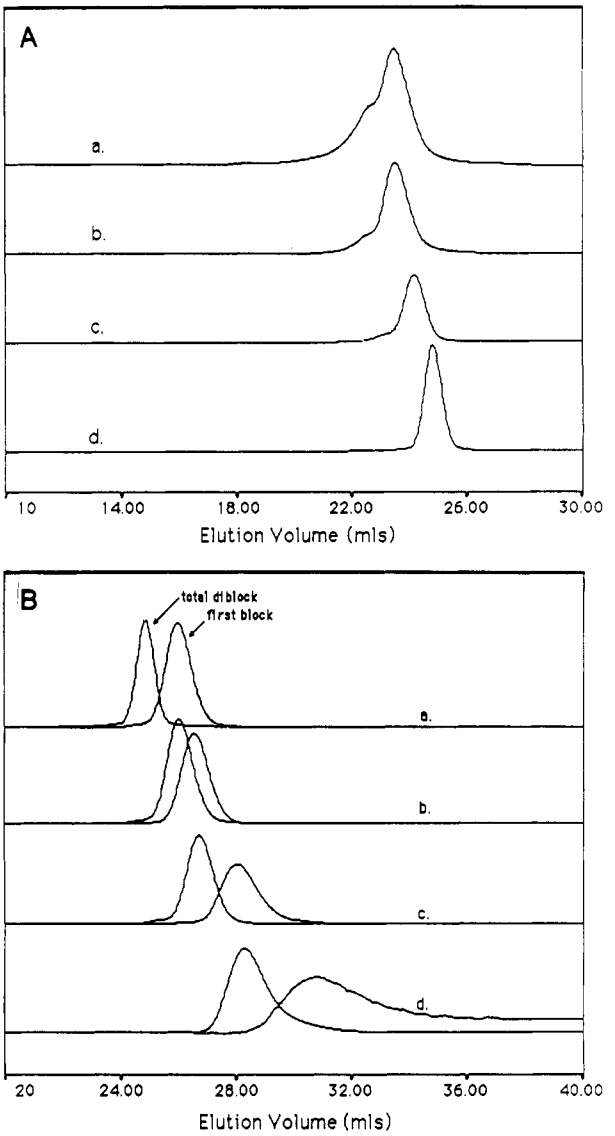

Figure 6. GPC traces of diblocks from Table II. (A) Constant molecular weight series (molecular weight 48 000): (a) 8% precursor (diblock 1); (b) 15% precursor (diblock 2); (c) 28% precursor (diblock 3); (d) 50% precursor (diblock 4). (B) Constant weight percent series (50 wt % precursor): (a) 48 000 (diblock 4); (b) 35 000 (diblock 5); (c) 20 000 (diblock 6); (d) 10 000 (diblock 7).

Table III
Morphological Characterization Results for Diblocks of System D: SAXS Results for the x, y, and z Directions

diblock	precursor state $d(x,y)$,[a] Å	precursor state $d(z)$,[b] Å	polyacetylene state $d(x,y)$,[a] Å	polyacetylene state $d(z)$,[b] Å	morphology
1	450	350	440	350	spherical
2	410		390		cylindrical
3	430	330	430		cylindrical
4		280		295	lamellar
5		230		245	lamellar
6		160			lamellar
7					

[a] x,y interdomain spacing. [b] z interdomain spacing.

GPC traces of these seven diblocks are shown in Figure 6; only traces of the total block are available for diblocks 1–3, and traces for both the first block and total block of the diblock are available for diblocks 4–7. SAXS patterns are shown in Figure 7 for diblocks 1–6, both for films in the precursor state and for films after the precursor was converted to polyacetylene. This figure shows SAXS patterns obtained with the X-ray beam aligned in the x

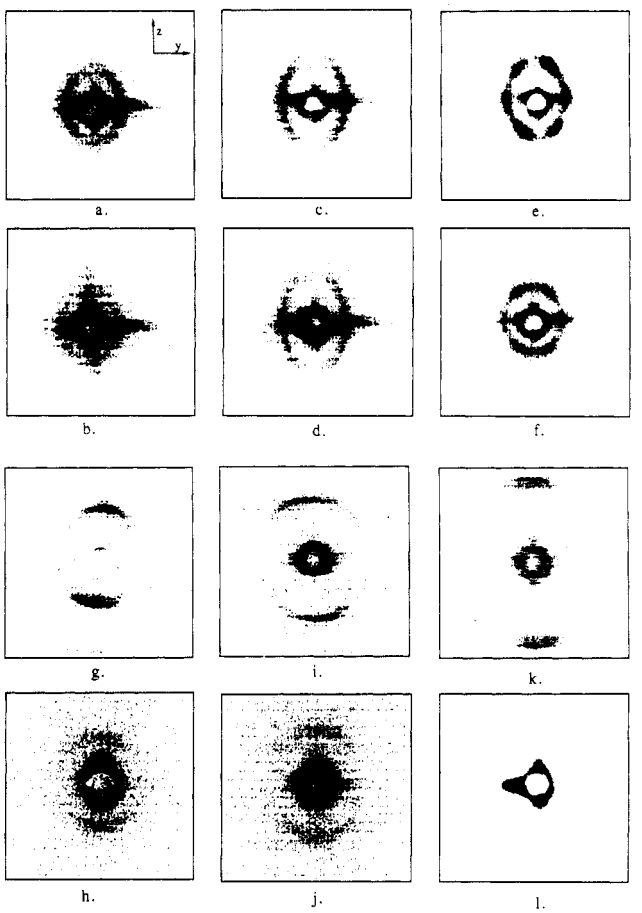

Figure 7. Small-angle X-ray scattering of diblocks 1–6 in Table II: (a) diblock 1 prior to conversion to polyacetylene; (b) diblock 1 after conversion to polyacetylene; (c) diblock 2 precursor; (d) diblock 2 converted; (e) diblock 3 precursor; (f) diblock 3 converted; (g) diblock 4 precursor; (h) diblock 4 converted; (i) diblock 5 precursor; (j) diblock 5 converted; (k) diblock 6 precursor; (l) diblock 6 converted. In pattern a the axes indicate the orientation of the y and z directions. The orientation is the same for patterns a–l.

direction of each of the different samples. Figure 8 shows scattering patterns for all three directions for diblocks 2 and 3 for both the precursor and converted polyacetylene diblocks. This figure is added to show a comparison of patterns for all the directions within a specific sample. TEM results are shown in Figure 9 for diblocks 3–6, again for both the precursor state and the polyacetylene state. X-ray fluorescence was used to map out the silicon content of an ultrathin section of diblock 4 in the precursor state. The results of this analysis are shown in Figure 10.

NMR and DSC were used to confirm the molecular weight ratios originally based on stoichiometry, and the results are consistent with stoichiometry. DSC can be used for this purpose by knowing the specific heat of formation of polyacetylene from its precursor (determined from a homopolymer sample) and then measuring the heat evolved for a diblock specimen of known weight.

Discussion

Originally, diblocks of system A were prepared, but the polymer of the precursor monomer (bis(trifluoromethyl)-tricyclo[4.2.2.0^{2,5}]deca-3,7,9-triene) was thermally unstable and converted substantially to polyacetylene over a 24-h period at room temperature. This thermal instability has been observed elsewhere,[27] and it makes casting uniform films difficult.

Introduction of the fused benzene ring to make the monomer benzotricyclo[4.2.2.0^{2,5}]deca-3,7,9-triene (re-

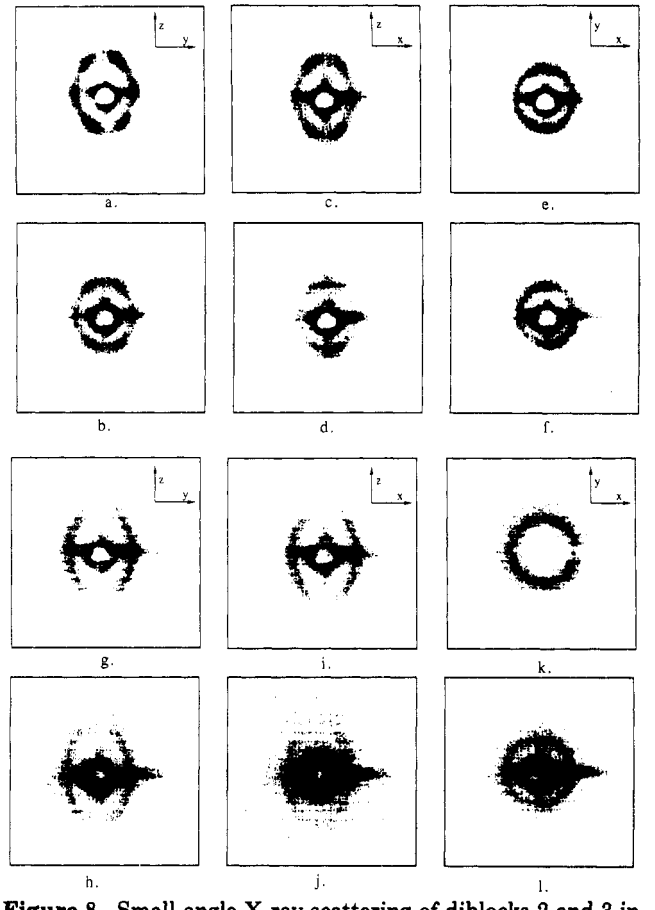

Figure 8. Small-angle X-ray scattering of diblocks 2 and 3 in Table II: (a–f) diblock 3 patterns; (g–l) diblock 2 patterns; (a,c,e,g,i,k) prior to conversion to polyacetylene; (b,d,f,h,j,l) after conversion to polyacetylene. The polyacetylene patterns have the same orientation as their corresponding precursor patterns.

ferred to hereafter as benz-precursor) caused the precursor polymer to become more stable at room temperature,[27] and it did not convert significantly to polyacetylene even over a period of a month. A few diblocks were made with norbornene and this benz-precursor, but none of these showed microphase separation (based on SAXS experiments).

To promote microphase separation, we attempted to increase the solubility parameter difference between the blocks of the copolymers.[1] Therefore a new precursor monomer was used: p-dimethoxybenzotricyclo[4.2.2.0^{2,5}]-deca-3,7,9-triene (referred to hereafter as pdmb-precursor), which contains the two methoxy groups on the fused benzene ring. As seen in the SAXS pattern in Figure 5, microphase separation does occur for this system, and the pattern indicates that the film has a lamellar morphology partially oriented parallel to the x–y plane, with an average interdomain spacing of 410 Å.

Using group contribution methods developed by Van Krevelin,[32] one can estimate solubility parameters for the various polymer repeat units present in the copolymers. The calculated values, with units of $J^{1/2}/cm^{3/2}$, are as follows: polynorbornene, 15.8; poly-benz-precursor, 18.3; poly-pdmb-precursor, 19.8. The solubility parameter difference for system B is thus 2.5 and for system C is 4. This supports the notion that the increased solubility parameter difference is responsible for microphase separation in system C.

To see microphase separation by TEM, we tried several different staining techniques, and none were successful.

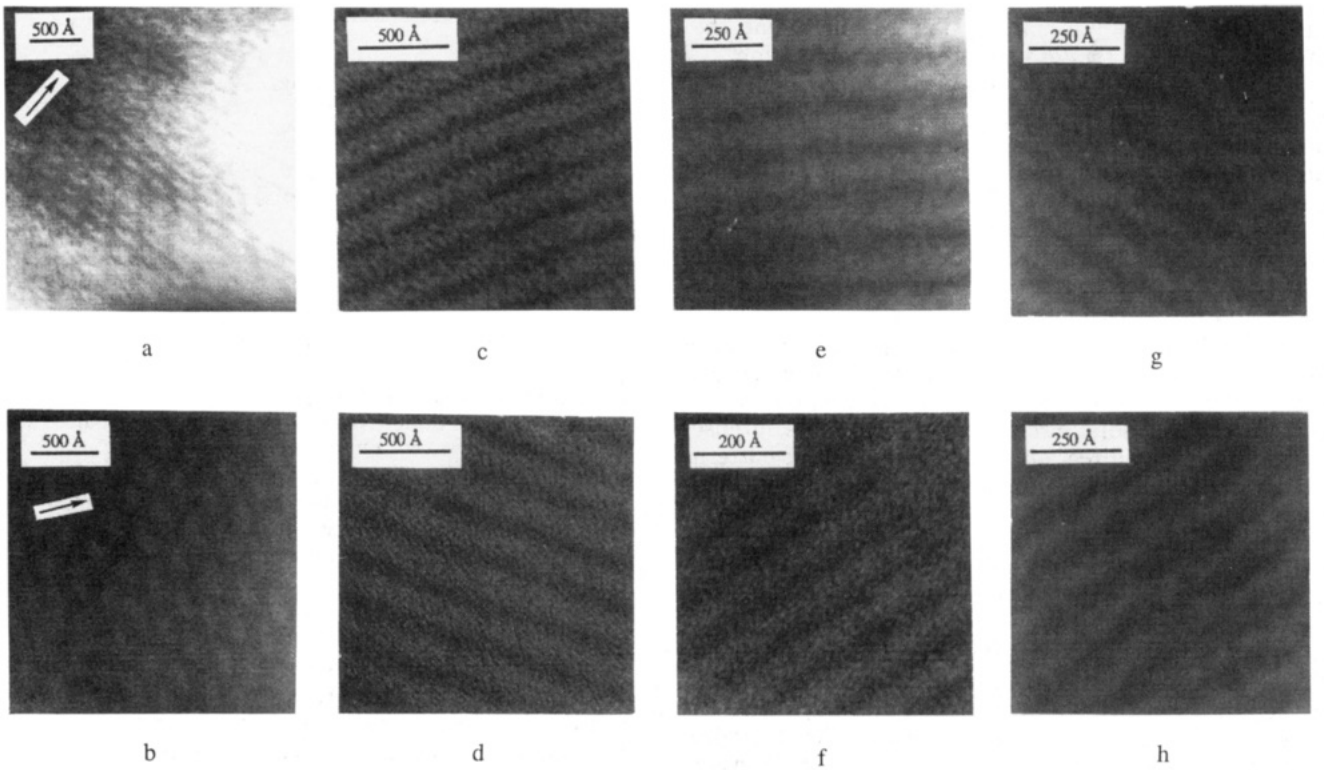

Figure 9. Transmission electron microscopy of diblocks 3–6 in Table II: (a) diblock 3 precursor; (b) diblock 3 converted; (c) diblock 4 precursor; (d) diblock 4 converted; (e) diblock 5 precursor; (f) diblock 5 converted; (g) diblock 6 precursor; (h) diblock 6 converted. In a and b the *z* direction is indicated by the direction of the arrow; in c–h the *z* direction is perpendicular to the lamellae.

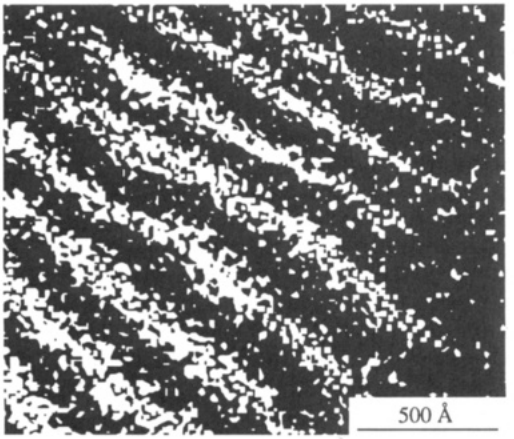

Figure 10. Silicon map of diblock 4 in Table II (50% precursor, molecular weight 48 000) in the precursor state using X-ray fluorescence with a scanning transmission electron microscope (computer enhanced to increase contrast). Silicon-rich areas appear as brighter regions.

It was desirable in our work to have a diblock system that would be observable by TEM as well as SAXS. To accomplish this, we derivatized the norbornene block to a ((trimethylsiloxy)methyl)norbornene (referred to hereafter as TMSO-norbornene) in the hope that contrast would be inherent to the system due to the presence of Si atoms. The TEM results in Figure 9 show clearly that this system does provide contrast, as long as the substituted norbornene block does not comprise more than ~75 wt % of the copolymer. The X-ray fluorescence results in Figure 10 confirm that the silicon-containing sequences are confined to clearly identifiable domains. Thus we can conclude that the alternating light and dark regions seen by TEM are alternating self-assembled structures of precursor polymer and poly-TMSO-norbornene.

A general observation about the SAXS patterns in Figures 7 and 8 is that most of them show an elliptical shape in the precursor state, with the major axis of the ellipse parallel to the *z* direction and the minor axis parallel to the *y* direction. Although the *y* direction patterns are not shown in Figure 7, in all cases the *y* direction scattering patterns for the precursor state are identical with those for the *x* direction; the *y* direction patterns also have the elliptical shape with the major axis in the *z* direction and the minor axis in the *x* direction. The *z* direction patterns, also not shown in Figure 7, either show nothing as in the case of diblocks 4–6 or show circles with no elliptical shape as in the case of diblocks 1–3. The major axis of the elliptical-shaped patterns being in the *z* direction suggests a closer packing of morphology in that direction. This fact is confirmed by the TEM picture in Figure 9a, where clearly the morphology shows a closer packing in the *z* direction. The fact that the packing of morphology is closer in the *z* direction than in the *x* and *y* directions implies that anisotropies inherent in the spin-casting process are reflected in the final specimen.

Another observation is that the SAXS and TEM results show that the diblock systems possessing microphase separation all exhibit long-range ordering, a quality which might be useful for electrical device fabrication. Although there is no flow field of the polymer solution relative to its container, it is presumed that the centrifugal forces resulting from the rotation of the cup and the free and wall surfaces all tend to promote long-range ordering of the morphologies in these systems.

In looking at the *x*, *y*, and *z* direction SAXS patterns for each specific diblock, we have attempted to infer a structure for them in the precursor state. For diblock 1, containing 8% precursor, Figure 7a shows a solid ellipse for scattering in the *x* direction; the *y* pattern is identical, and the *z* pattern shows a solid circle (the *y* and *z* patterns are not shown). This would indicate the existence of spherical morphology, with the packing being shorter in the *z* direction. TEM results are not available for this

diblock because it was not possible to microtome the material to obtain sections suitable for examination.

For diblock 2 in the precursor state, patterns g, i, and k of Figure 8 show scattering patterns for the x, y, and z directions, respectively. The patterns for the x and y directions show arcs of an ellipse, whereas the z direction pattern shows a solid circle. These three patterns taken together suggest the presence of a meandering cylindrical morphology, mainly oriented with the axes parallel to the z direction. Unfortunately, TEM pictures could not be obtained for this particular copolymer.

Diblock 3 shows a very interesting SAXS pattern (Figure 8a,c,e) in the precursor state. The x and y patterns show three pairs of dots spaced around an ellipse, and the z pattern shows a solid circle with slightly more intense scattering in the y direction. We believe that this pattern can be attributed to a morphology of hexagonally packed cylinders. The fact that the pattern is similar between the x and y directions but slightly more intense for the x direction (Figure 8a,c) indicates that the cylinders lie in various directions in the x–y plane, with orientation of the axes toward the x direction being slightly favored over those of the y direction. If this is the case, the z direction should give a circle with slightly more intense scattering in the y direction, which is the observed result. Figure 9a shows the TEM picture of this diblock. The structure seen suggests the presence of cylinders that have been cut at an angle and that there is some deformation associated with the microtoming process; nevertheless, the hexagonal arrangement can be visualized in this picture. Other areas of the same sample showed parallel lines in the electron microscope; the existence of these two structures in the same sample further corroborates the existence of cylinders of varying orientation (in the x–y plane). Furthermore, the percent of precursor in this diblock falls within the range typically associated with cylindrical morphology.

For precursor diblocks 4, 5, and 6, the SAXS patterns in the x direction all show one pair of arcs. The patterns in the y direction are identical, and none of the z direction patterns show any scattering. These patterns indicate that in all three samples the morphology is lamellar, with the lamellae being essentially parallel to the x–y plane. These lamellar structures are clearly visible in the micrographs shown in Figure 9c,e,g.

Precursor diblocks 1–6 were all heat treated to form the polyacetylene diblocks, and in all but one sample, diblock 6, the microphase separation was retained. In diblocks 1 and 2 (Figure 7b,d) the nature of the spherical or cylindrical morphology of the precursor is preserved in the heat-treated materials. Patterns a–f of Figure 8 show that for diblock 3 microphase separation is retained, but the nature of the structure changes slightly upon conversion to polyacetylene. The patterns suggest that the packing distances become more uniform among the x, y, and z directions. Also, the patterns show that the cylindrical axes tend to orient even more in the x direction, giving rise to a change in the y pattern (Figure 8c,d) from three pairs of dots to one pair of dots. The TEM picture in Figure 9b further substantiates retention of structure and more uniform packing after conversion to polyacetylene for diblock 3.

In diblocks 4 and 5, the original structure is retained, but the interdomain spacing increases somewhat upon conversion to polyacetylene, based on SAXS results in Figure 7g–j. The small increase in domain spacing arises when the lamellar morphology is allowed to rearrange toward its equilibrium spacing during the heating process; in addition, the evolution of the aromatic fragment from the precursor repeat unit might account for some free

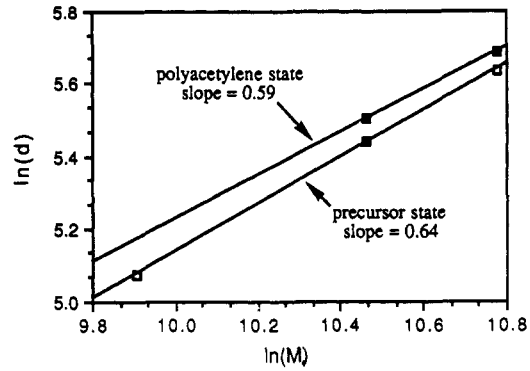

Figure 11. log–log plot of interdomain spacing (SAXS) vs molecular weight for diblocks 4–6 (Table II) in the precursor state and for diblocks 4 and 5 in the polyacetylene state.

volume increase and a corresponding increase in the domain spacing. The micrographs in Figure 9d,f substantiate the fact that lamellar microphase separation is retained for diblocks 4 and 5 upon conversion to polyacetylene.

In diblock 6 the lamellar structure apparently disappears upon conversion to polyacetylene, based on the SAXS result in Figure 7l. This can be explained by the fact that this particular diblock is close to the boundary separating the heterogeneous and homogeneous regimes for this diblock system; it is possible that upon heating, the new polyacetylene-containing diblock exists in the homogeneous regime, thus showing no microphase separation. On the other hand, some structure is seen by TEM (Figure 9h).

It is interesting to note here that the lamellar domain spacing for diblocks 4–6 decreases as the molecular weight decreases. This is what would be expected, and Hashimoto has described scaling laws for such lamellar systems;[7] the domain spacing (d) is expected to depend on the $^2/_3$ power of the block copolymer molecular weight. Figure 11 shows a plot of lamellar spacing vs molecular weight for several of our diblocks. The slope is 0.64 for the lamellar diblocks in the precursor state and 0.59 for the two lamellar diblocks in the polyacetylene state. On the basis of this small amount of data we conclude that the novel systems examined here follow reasonably well the standard scaling laws for amorphous diblock copolymers, thereby providing some materials design guidance for the thickness and separation of the self-assembled layers of polyacetylene.

Diblock 7, containing 50 wt % pdmb-precursor block with a total molecular weight of 10 000, showed no microphase separation (SAXS), and it was clearly different in physical handling compared to the other films cast in the same way. We conclude therefore that diblock 7 is homogeneous. This piece of information enables us to locate a homogeneous/heterogeneous boundary in a qualitative phase diagram such as the one shown in Figure 12. The spherical, cylindrical, and lamellar regions are divided by boundaries which are in the same range of composition reported for more conventional diblocks. Again the success in describing the precursor diblocks with a qualitative phase diagram is useful for a rational design of materials containing nanoscale regions of polyacetylene.

Finally, the possible range of vertical locations of the phase diagram boundary in Figure 12 is limited by the molecular weights of diblocks 6 and 7. From earlier theoretical work[33] it is known that the product of the repeat unit interaction parameter and the total degree of polymerization of the diblock is $\chi N = 10.5$ at the minimum of the phase diagram boundary. The data of Figure 12

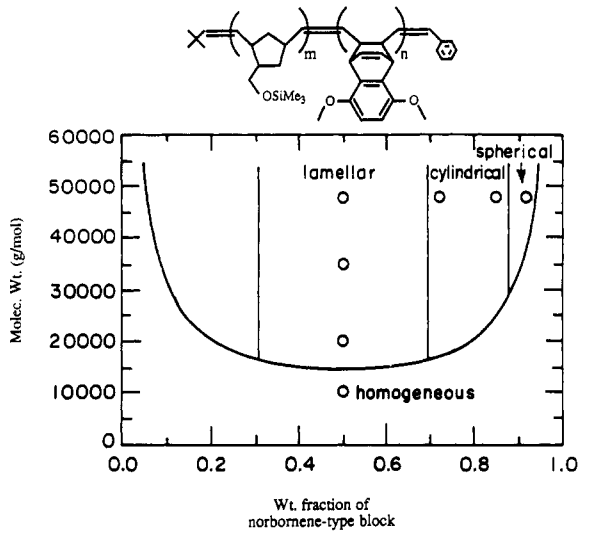

Figure 12. Qualitative phase diagram of poly[((trimethylsiloxy)-methyl)norbornene]/poly-pdmb-precursor diblocks at room temperature.

lead to values of χ for the repeat units of system D between 0.11 and 0.23. This value can be compared to a χ value of 0.02 for diblocks of polystyrene–polybutadiene,[34] which is one of the more frequently studied diblock copolymer systems.

Conclusion

The Durham route to polyacetylene provides a convenient method to incorporate polyacetylene into diblock copolymers. The results presented in this paper clearly show that self-assembled structures of polyacetylene are obtainable through this precursor route in a variety of morphologies. The lamellar morphologies obey well-established scaling laws for amorphous diblock systems. The necessity of using "derivatized" monomers is seen in the fact that microphase separation was observed only after the ether groups were added to the precursor monomer. Derivatized norbornene is not essential but is convenient for providing observable TEM results.

The five diblocks possessing self-assembled polyacetylene structures (diblocks 1–5) can now be chemically doped to render them electrically conductive and thus create materials with potentially interesting electrical properties. Such work is in progress and results will be the subject of a forthcoming paper.

Acknowledgment. This work has been supported by NSF/MRL under Grant DMR-87-19217, through the CMSE at MIT. Special thanks are extended to Melanie Lazaro, an undergraduate research assistant, for her work on the synthesis of the pdmb-precursor monomer.

References and Notes

(1) Helfand, E.; Wasserman, Z. R. *Developments in Block Copolymers—2*; Goodman, I., Ed.; Applied Science Publishers: New York, 1982; pp 99–125.
(2) *Langmuir–Blodgett Films*; Roberts, G., Ed.; Plenum Press: New York, 1990.
(3) Sailor, M. J.; Ginsburg, E. J.; Gorman, C. B.; Kamur, A.; Grubbs, R. H.; Lewis, N. S. *Science* **1990**, *249*, 1146.
(4) Alward, D. B.; Kinning, D. J.; Thomas, E. L.; Fetters, L. J. *Macromolecules* **1987**, *20*, 2940.
(5) Folkes, M. J.; Keller, A. *Polymer* **1971**, *12*, 222.
(6) Bates, F. S.; Cohen, R. E.; Berney, C. V. *Macromolecules* **1982**, *15*, 589.
(7) Hashimoto, T. *Macromolecules* **1982**, *15*, 1548.
(8) Hong, K. M.; Noolandi, J. *Macromolecules* **1981**, *14*, 736.
(9) Leibler, L. *Macromolecules* **1980**, *13*, 1602.
(10) Bolognesi, A.; Catellani, M.; Destri, S. *Mol. Cryst. Liq. Cryst.* **1985**, *117*, 29.
(11) Kminek, I.; Trekoval, J. *Makromol. Chem., Rapid Commun.* **1984**, *5*, 53.
(12) Bates, F. S.; Baker, G. L. *Macromolecules* **1983**, *16*, 707.
(13) Bolognesi, A.; Porzio, W.; Catellani, M.; Destri, S. *Mol. Cryst. Liq. Cryst.* **1985**, *117*, 71.
(14) Bolognesi, A.; Catellani, M.; Destri, S.; Porzio, W. *Polymer* **1986**, *27*, 1128.
(15) Meille, S. V.; Pedemonte, E. *Makromol. Chem.* **1986**, *187*, 1287.
(16) Armes, S. P.; Vincent, B.; White, J. W. *J. Chem. Soc., Chem. Commun.* **1986**, 1525.
(17) Galvin, M. E.; Wnek, G. E. *Mol. Cryst. Liq. Cryst.* **1985**, *117*, 33.
(18) Kanga, R. S.; Hogen-Esch, T. E.; Randrianalimanana, E.; Soum, A.; Fontanille, M. *Macromolecules* **1990**, *23*, 4235, 4241.
(19) Aldissi, M.; Bishop, A. R. *Polymer* **1985**, *26*, 622.
(20) Krouse, S. A.; Schrock, R. R. *Macromolecules* **1988**, *21*, 1888.
(21) Baker, G. L.; Bates, F. S. *Mol. Cryst. Liq. Cryst.* **1985**, *117*, 15.
(22) Aldissi, M. *Mol. Cryst. Liq. Cryst.* **1990**, *180A*, 9.
(23) Gilliom, L. R.; Grubbs, R. H. *J. Am. Chem. Soc.* **1986**, *108*, 733.
(24) Wallace, K. C.; Schrock, R. R. *Macromolecules* **1987**, *20*, 448.
(25) Schrock, R. R.; Krouse, S. A.; Knoll, K.; Feldman, J.; Murdzek, J. S.; Yang, D. C. *J. Mol. Catal.* **1988**, *46*, 243.
(26) (a) Schrock, R. R.; Feldman, J.; Grubbs, R. H.; Cannizzo, L. *Macromolecules* **1987**, *20*, 1169. (b) Schrock, R. R. *Acc. Chem. Res.* **1990**, *23*, 158.
(27) Edwards, J. H.; Feast, W. J.; Bott, D. C. *Polymer* **1984**, *25*, 395.
(28) Liu, R. S. H.; Krespan, C. G. *J. Org. Chem.* **1969**, *34*, 1271.
(29) Paquette, L. A.; Kukla, M. J.; Stowell, J. C. *J. Am. Chem. Soc.* **1972**, *94*, 4920.
(30) Reppe, W.; Schlichting, O.; Klager, K.; Toepel, T. *Justus Liebigs Ann. Chem.* **1948**, *560*, 1.
(31) Bates, F. S.; Cohen, R. E.; Argon, A. S. *Macromolecules* **1983**, *16*, 1108.
(32) Van Krevelin, D. W. *Properties of Polymers: Their Estimation and Correlation with Chemical Structure*; Elsevier Scientific Publishing Company: New York, 1976; pp 129–150.
(33) Leibler, L. *Makromol. Chem., Rapid Commun.* **1981**, *2*, 393.
(34) Narasimhan, V.; Huang, R. Y. M.; Burns, C. M. *J. Polym. Sci., Polym. Phys. Ed.* **1983**, *21*, 1993.

Registry No. System A (copolymer), 117223-70-8; system B (copolymer), 135710-35-9; system C (copolymer), 135710-36-0; system D (copolymer), 135710-?7-1; TMSCl, 75-77-4; 5-norbornene-2-methanol, 95-12-5; ((trimethylsiloxy)methyl)norbornene, 121949-44-8.